Toxicology 334 (2015) 72–80

Contents lists available at ScienceDirect

Toxicology

journal homepage: www.elsevier.com/locate/toxicol

PINK1/Parkin-mediated mitophagy alleviates chlorpyrifos-induced apoptosis in SH-SY5Y cells

Hongmei Dai[a], Yuanying Deng[a], Jie Zhang[b], Hailong Han[c], Mingyi Zhao[a], Ying Li[a], Chen Zhang[a], Jing Tian[a], Guoying Bing[d], Lingling Zhao[a,*]

[a] Department of Pediatrics, the Third Xiangya Hospital of Central South University, Changsha, Hunan Province, China
[b] Department of Neurology, the Second Xiangya Hospital of Central South University, Changsha, Hunan Province, China
[c] State Key Laboratory of Medical Genetics, Central South University, Changsha, Hunan Province, China
[d] Department of Anatomy and Neurobiology, University of Kentucky, School of Medicine, Lexington, KY, USA

ARTICLE INFO

Article history:
Received 8 April 2015
Received in revised form 4 June 2015
Accepted 5 June 2015
Available online 9 June 2015

Keywords:
Apoptosis
Chlorpyrifos
Mitophagy
PINK1/Parkin

ABSTRACT

Chlorpyrifos (CPF) is one of the most widely used organophosphorous insecticides. There are links between CPF exposure and neurological disorders. Mitochondrial damage has been implicated to play a key role in CPF-induced neurotoxicity. Mitophagy, the selective autophagic elimination of mitochondria, is an important mitochondrial quality control mechanism. However, the role of mitophagy in CPF-induced neurotoxicity remains unclear. In this study, CPF-caused mitochondrial damage, role and mechanism of mitophagy on CPF-induced neuroapoptosis were extensively studied by using SH-SY5Y cells. We showed that CPF treatment caused mitochondrial fragmentation, excessive ROS generation and mitochondrial depolarization, thus led to cell apoptosis. Moreover, CPF treatment also resulted in increased colocalizaton of mitochondria with LC3, decreased levels of mitochondrial proteins, PINK1 stabilization and mitochondrial accumulation of Parkin. These data suggested that CPF treatment induced PINK1/Parkin-mediated mitophagy in SH-SY5Y cells. Furthermore, knockdown of Parkin dramatically increased CPF-induced neuroapoptosis. On the other hand, overexpression of Parkin markedly alleviated CPF-induced SH-SY5Y cell apoptosis. Together, these findings implicate a protective role of PINK1/Parkin-mediated mitophagy against neuroapoptosis and that enhancing mitophagy provides a potential therapeutic strategy for CPF-induced neurological disorders.

1. Introduction

Prospective cohort studies have shown that prenatal or early childhood exposure of chlorpyrifos (CPF) causes adverse neurodevelopmental outcomes, such as decreased head circumference, poorer intellectual development and cognitive deficits, mental and motor delays, as well as neurodegenerative diseases (Bouchard et al., 2011; Engel et al., 2007, 2011; Eskenazi et al., 2007; Freire and Koifman 2012; Rauh et al., 2011; Whyatt et al., 2004). Experimental studies have demonstrated that CPF exposure results in inhibition of DNA synthesis, induces apoptosis and leads to adverse neurodevelopmental problems (Aldridge et al., 2005; Canadas et al., 2005; Gupta et al., 2010; Lee et al., 2012; Qiao et al., 2001; Saulsbury et al., 2008).

Yet, the underlying mechanism of neurotoxicology induced by CPF exposure remains not fully defined. Mitochondria are the major cellular source of excessive reactive oxygen species (ROS) and are also vulnerable targets of ROS (Cho et al., 2010; Liesa et al., 2009). Excessive mitochondrial ROS production leads to oxidative damage to cellular components including mitochondrial proteins, lipids and DNA, which in turn enhances ROS production and further mitochondria damage, forming a vicious cycle. Mitochondrial damage leads to the release of proapoptotic proteins, such as cytochrome c (cyt c), resulting in cell apoptosis. It was reported that CPF exposure caused apoptosis in dopaminergic neuronal components PC12 cells through inducing mitochondrial dysfunction and excessive generation of ROS (Lee et al., 2012). This indicates that mitochondrial damage and excessive ROS generation may play an important role in CPF-induced neuroapoptosis. So,

Abbreviations: CCCP, carbonyl cyanide *m*-chlorophenyl hydrazone; CCK-8, cell counting kit-8; CPF, chlorpyrifos; DMSO, dimethyl sulfoxide; LC3, microtubule-associated protein 1 light chain 3; NDUFS3, nicotinamide adenine dinucleotide dehydrogenase Fe-S protein 3; ROS, reactive oxygen species; PINK1, PTEN-induced putative kinase 1.

* Corresponding author at: Department of Pediatrics, the Third Xiangya Hospital of Central South University, 138, Tongzipo Road, Yuelu District Changsha, Hunan Province 410013, China. Fax: +86 731 88618498.
E-mail address: llzhao2011@qq.com (L. Zhao).

http://dx.doi.org/10.1016/j.tox.2015.06.003

removal of damaged mitochondria may play a protective role in CPF-induced cytotoxicity.

Mitophagy, the selective elimination of mitochondria via autophagy, is an important mechanism of mitochondrial quality control in physiological and pathological conditions. Defects in mitophagy have been implicated in a variety of human disorders. The best well-known signaling pathway of mitophagy is regulated by PTEN-induced putative kinase 1 (PINK1) and Parkin. In healthy mitochondria, PINK1 is constitutively translocated into mitochondria and cleaved by protease Parl1 on mitochondrial inner membrane (Jin et al., 2010; Meissner et al., 2011). When a subset of mitochondria become impaired and depolarized, PINK1, which acts as a molecular sensor of damaged mitochondria, is prevented from importing into mitochondria and consequently accumulated on mitochondrial outer membrane, which in turn recruits Parkin from cytosol to the damaged mitochondria (Matsuda et al., 2010; Meissner et al., 2011). Once recruited, Parkin ubiquitinates various substrates, thus results in the induction of autophagic removal of damaged mitochondria (Narendra et al., 2008). Accumulating evidences have demonstrated that mitochondrial fragmentation is required for activation of mitophagy. However, mitochondrial fragmentation itself is not enough to induce mitophagy, which needs some other factors, such as ROS generation and mitochondrial depolarization (Frank et al., 2012; Matsuda et al., 2010). Whether CPF exposure also induces mitophagy remains unclear. Although Park et al. (2013) have shown that enhancement of autophagy by rapamycin alleviates CPF-induced apoptosis, whether mitophagy contributes to the protective effect of autophagy on CPF induced cell death remains unknown.

In the present study, we use SH-SY5Y cells as an in vitro model to determine the role and regulatory mechanism of mitophagy in CPF-induced neurotoxicity. In this study, we found that CPF exposure decreased cell viability, increased apoptosis, and induced mitophagy. Further exploration showed that mitophagy played a cytoprotective role in CPF-induced apoptosis, and PINK1/Parkin signaling was involved in CPF-induced mitophagy.

2. Materials and methods

2.1. Reagents and antibodies

CPF was obtained from Sigma–Aldrich, and dissolved in dimethyl sulfoxide (DMSO). Dulbecco's modified Eagle's medium (DMEM)/F12 (1:1), fetal bovine serum (FBS), sodium pyruvate, L-glutamine, penicillin–streptomycin and trypsin–EDTA were obtained from Gibco. Primary antibodies against caspase-3, cleaved caspase-3 and LC3 (microtubule-associated protein 1 light chain 3) were purchased from Cell Signaling Technology. Primary antibodies against TIM23 and nicotinamide adenine dinucleotide dehydrogenase Fe-S protein 3 (NDUFS3) were obtained from Abcam. PINK1 and glyceraldehyde-3-phosphate dehydrogenase (GAPDH) antibodies were obtained from Novus and Sigma, respectively. Tetramethylrhodamine ethyl ester (TMRE) was purchased from Molecular Probes (Eugene, OR).

2.2. Cell culture and treatment

SH-SY5Y cells were obtained from American Type Culture Collection (ATCC, Rockville, MD, USA), and grown in DMEM/F12 medium supplemented with 10% FBS, 1% penicillin–streptomycin (100 U/ml of penicillin G and 100 mg/ml of streptomycin), 1% glutamine and 1% sodium pyruvate. To avoid possible inhibition of CPF by serum proteins, cells were treated with CPF, which were dissolved in medium with 1% fetal bovine serum.

2.3. Generation of constructs and siRNA oligonucleotides

PINK1-flag, myc-Parkin and Parkin-GFP were generated by PCR amplification and standard subcloning. To generate PINK1-flag plasmids, cDNA of human PINK1 was amplified and then inserted between BamH1/HindIII of pcDNA3.1 myc his A (−) (Invitrogen). A flag tag sequence was added to the reverse primer of PINK1. Similarly, human PARK2 cDNA was amplified and inserted between EcoR1/HindIII of pcDNA3.1 myc his A (−) (Invitrogen). A myc tag sequence was added to the forward primer of PARK2. The Parkin-GFP-N1 plasmid was generated by inserting PARK2 cDNA between BamH1/EcoR1 of pEGFP-N1 (Clontech). pDsRed2-Mito was purchased from Clontech. Plasmid LC3-GFP-N1 was purchased from Addgene.

Human Parkin siRNA (target sequence: 5′-GGCCTGG GCTGTGGGTTTGCC-3′) and control siRNA oligonucleotides were purchased from Shanghai GenePharma.

2.4. Cell viability assay

The cell viability of SH-SY5Y cells was assayed by using cell counting kit-8 (CCK-8, DoJinDo Molecular Technology Inc.) according to the instruction. Cells were seeded in 96-well plates at 37 °C in humidified 5% CO_2 atmosphere. After incubation with CPF for 6, 12, 24 or 48 h, 10 μl of CCK-8 solution was added into each well and then incubated for another 4 h. The absorbance at 450 nm was spectrophotometrically measured using a microplate ELISA reader (Synergy HT, Bio-TEK, US). SH-SY5Y cells cultured in DMEM/F 12 medium treated by 0.1% DMSO and culture media without cells were used as negative and blank controls, respectively. Following the deduction of the blank cell absorbance, the proliferation rate was expressed as a percentage of the absorbance to control cell absorbance.

2.5. Measurement of intracellular ROS

The conversion of non-fluorescent chloromethyl-DCFDA to fluorescent DCF was used to monitor intracellular ROS production according to the instruction. SH-SY5Y cells growing in 24 well plates were treated with CPF at a concentration of 100 μM or DMSO as a control for 6 h. Cells were washed once with PBS, then incubated in 1× buffer containing 10 uM DCFDA for 30 min at 37 °C in the dark, and subsequently washed with PBS to remove excess dye. DCFDA intensity was then detected by ELISA reader (Ex: 485 nm, Em: 535 nm).

2.6. Mitochondrial membrane potential ($\Delta\Psi m$) assay

TMRE Mitochondrial Membrane Potential Assay Kit (Abcam) was used to measure $\Delta\Psi m$ of SH-SY5Y cells according to the instruction. SH-SY5Y cells growing in 96-well plates were loaded with 200 nM TMRE (Molecular Probe) for 15 min at 37 °C. Cells were washed once with 0.2% BSA in PBS and then read on a fluorescence plate reader with settings suitable for TMRE (Ex: 549 nm, Em: 575 nm).

2.7. Line profiles analysis

Line profiles from the two fluorescent channels were analyzed by using the Image J red–green–blue (RGB) Profiler plug-in (Pidoux et al., 2011). Briefly, cells were transfected for LC3-GFP together with mito-Dsred, and the fixed cells on the coverslip were treated with CPF or DMSO as a control. And multiple-channel line profiles were drawn for the same particle in the corresponding merged image. The line profile implies the distribution of the two fluorophores on the given line analyzed.

2.8. Live-cell imaging

Cells grown in a 20 mm Glass bottom plate (catalog no. 801008, NEST) were co-transfected with 1 μg pDsRed2-Mito and 1 μg Parkin-GFP. 24 h after transfection, pDsRed2-Mito and Parkin-GFP positive cells were recorded at 90 s/interval at 37 °C, humidified 5% CO_2 for 3 h using confocal microscopy (Leica) with a ×100 objective lens plus × amplification by the software Leica Application Suite Advanced Fluorescence (LASAF). To minimize phototoxicity, the red channel and green channel were imaged. Kymographs were generated with the Multi Kymograph plug-in of the Image J software according to the instructions of J. Rietdorf, European Molecular Biology Laboratory, Heidelberg, Germany.

2.9. Cell counting analysis

To quantitate CPF-induced mitochondrial fragmentation, the number of cells with fragmented mitochondrial and total cells in three random vision fields, each of which contains >100 cells, were counted. The number of cells with fragmented mitochondria was normalized to total cells. Three independent experiments were performed. To quantitate CPF-induced mitophagy, the number of cells showing colocalization between mito-DsRed and Parkin-GFP was counted and normalized to the number of cells expressing both mito-DsRed and Parkin-GFP. In each experiment, >200 cells expressing both mito-DsRed and Parkin-GFP were calculated, and three independent experiments were done. Similarly, the number of cells showing colocalization between mito-DsRed and LC3-GFP was counted and normalized to the total number of cells expressing both mito-DsRed and LC3-GFP. In each experiment, >200 cells expressing both mito-DsRed and LC3-GFP were calculated, and three independent experiments were done.

2.10. Statistical analysis

Dates are expressed as mean ± SE. The significance of variation among different groups was determined by one-way ANOVA followed by Dunnett's multiple-comparison test. Difference between the experimental group and the control group were determined by Student's *t*-test. $p < 0.05$ was considered statistically significant.

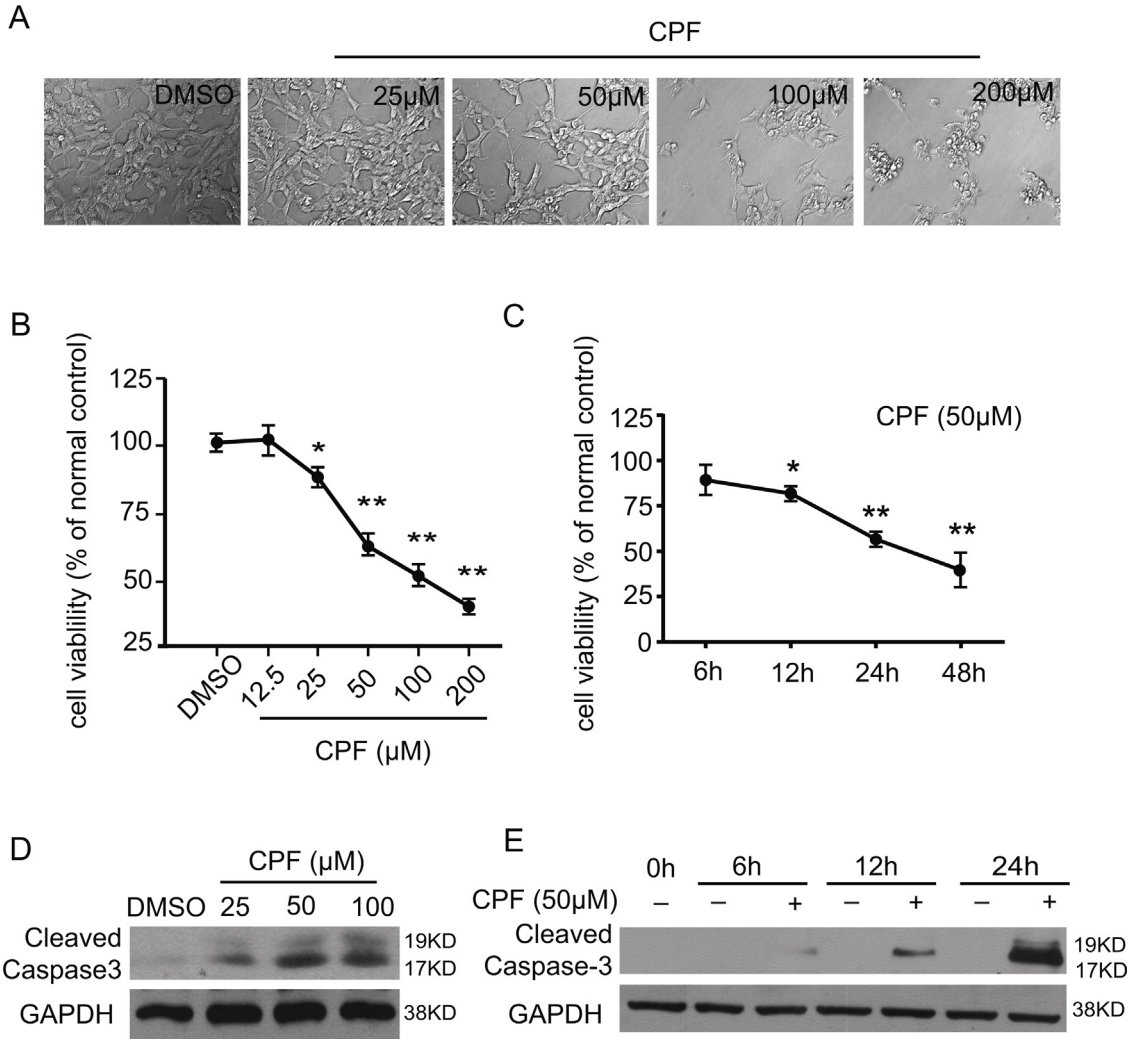

Fig. 1. CPF treatment causes neurotoxicity in SH-SY5Y cells.
(A) Representative images (20×). SH-SY5Y cells were treated with various concentrations of CPF for 24 h. Cell morphology was observed by using contrast microscopy. DMSO represents the vehicle. (B, C) Cell viability was measured by CCK-8 assay ($n = 5$). (D, E) Western blot analysis of the expression of cleaved caspase-3 ($n = 3$). Cells were treated with various concentration of CPF for indicated time course, and then whole cell lysates were collected for western blot analysis. Data in panels B is expressed as mean ± SE ($n = 5$). $^{*}p < 0.05$, $^{**}p < 0.01$, with the respect to the control cells (DMSO).

3. Results

3.1. CPF treatment induces apoptotic cell death in SH-SY5Y cells

To determine whether CPF has neurotoxic effects, SH-SY5Y cells were treated for 24 h with various concentrations of CPF. Microscopic observations showed dramatic morphological changes and a significant decrease in the number of SH-SY5Y cells in response to CPF treatment (Fig. 1A). CCK-8 assay was performed to evaluate cell viability. Similarly, CPF caused a concentration- (Fig. 1B) and time-dependent (Fig. 1C) decrease in cell viability. To determine whether CPF induces apoptosis, we determined the activation of cleaved caspase-3 by western blot analysis. As show in Fig. 1E and F, CPF treatment induced a concentration- and time-dependent expression of cleaved caspase-3, suggesting the activation of caspase-3. Collectively, these results suggest that CPF treatment causes cell apoptosis in SH-SY5Y cells.

3.2. CPF induces mitochondrial damage and ROS generation in SH-SY5Y cells

Mitochondrial morphology was determined by immunofluorescence staining with an antibody against mitochondrial protein TIM23. As shown in Fig. 2A, mitochondria in control cells were filamentous with a tubular or thread-like appearance and were often interconnected to form a network. But after 50 μM CPF exposure for 24 h, the mitochondrial networks in of SH-SY5Y cells were broken down and fragmented into short rods or spheres. Cell counting revealed that >75% cells that were exposed to CPF contained fragmented mitochondria (Fig. 2B). Moreover, we determined the effect of CPF on ROS generation. As shown in Fig. 2C, CPF exposure dramatically increased the signals of fluorescent DCF, suggesting an increase in ROS generation. In addition, we determined the membrane potential of mitochondria in SH-SY5Y cells exposed to CPF via TMRE staining, As shown in Fig. 2D. Quantitative analysis

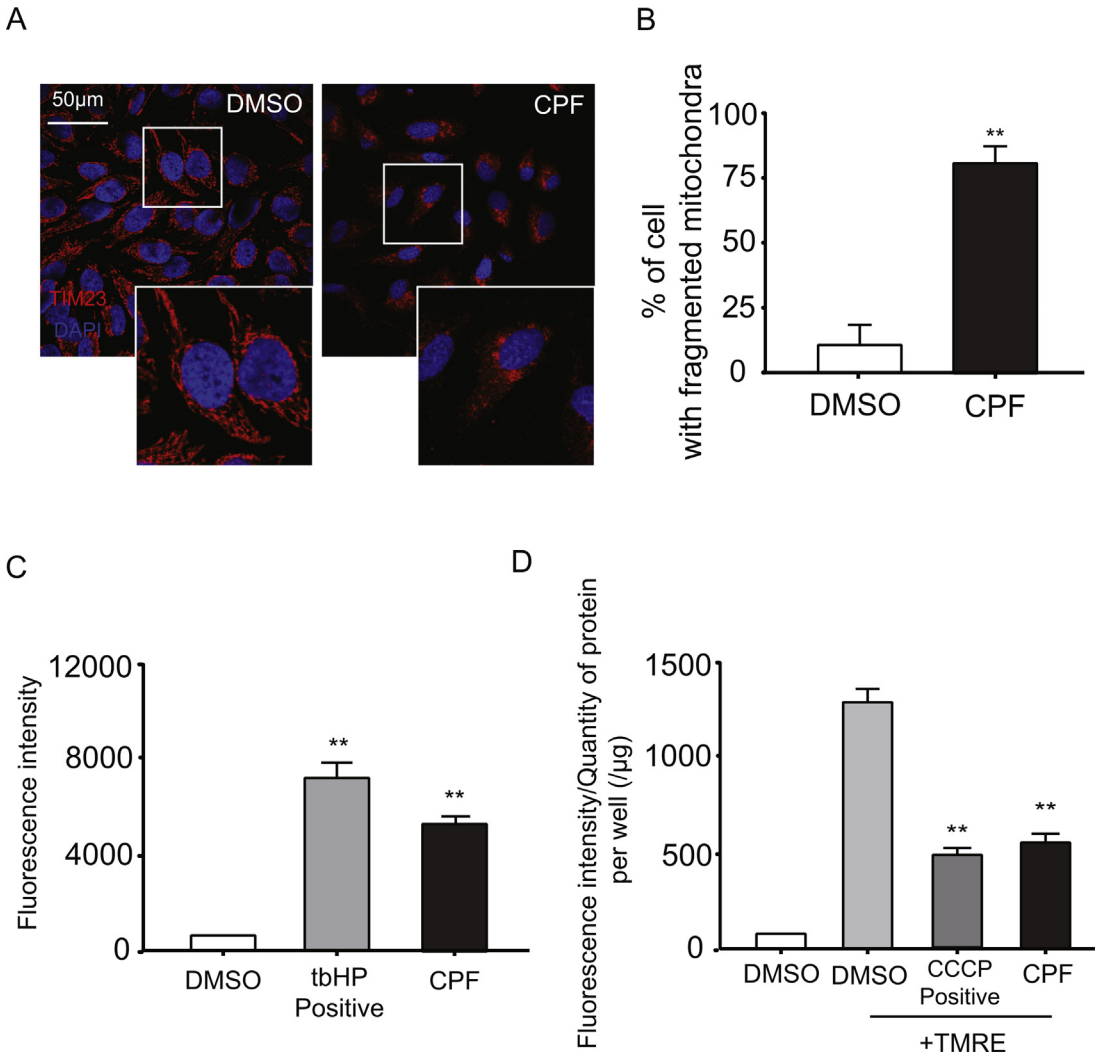

Fig. 2. Effect of CPF exposure on mitochondria and ROS generation.
(A) Representative images of mitochondria (Scale bars, 50 μm). SH-SY5Y cells were treated with 50 μM CPF for 24 h. Then, cells were fixed and stained with anti-TIM23 antibody to label mitochondria. DAPI staining was performed to label nuclear. Flourescence images were taken by Leica confocal microscope. (B, C and D) SH-SY5Y cells were treated with 50 μM CPF for 6 h. (B) Quantitative analysis of SH-SY5Y cells with fragmented mitochondria ($N = 3$, $n > 100$). (C) Quantitative analysis of intracellular ROS generation. Cells were stained with DCFDA and the density of fluorescent signals was measured. 10 μM tbHP for 2 h as a positive control. (D) Quantitative analysis of mitochondrial membrane's potential. The cells were stained with TMRE, and the density of fluorescent signals was analyzed and normalized to protein quantity, 20 μM CCCP for 2 h as a positive control. $^{**}p < 0.01$, with the respect to the control cells (DMSO).

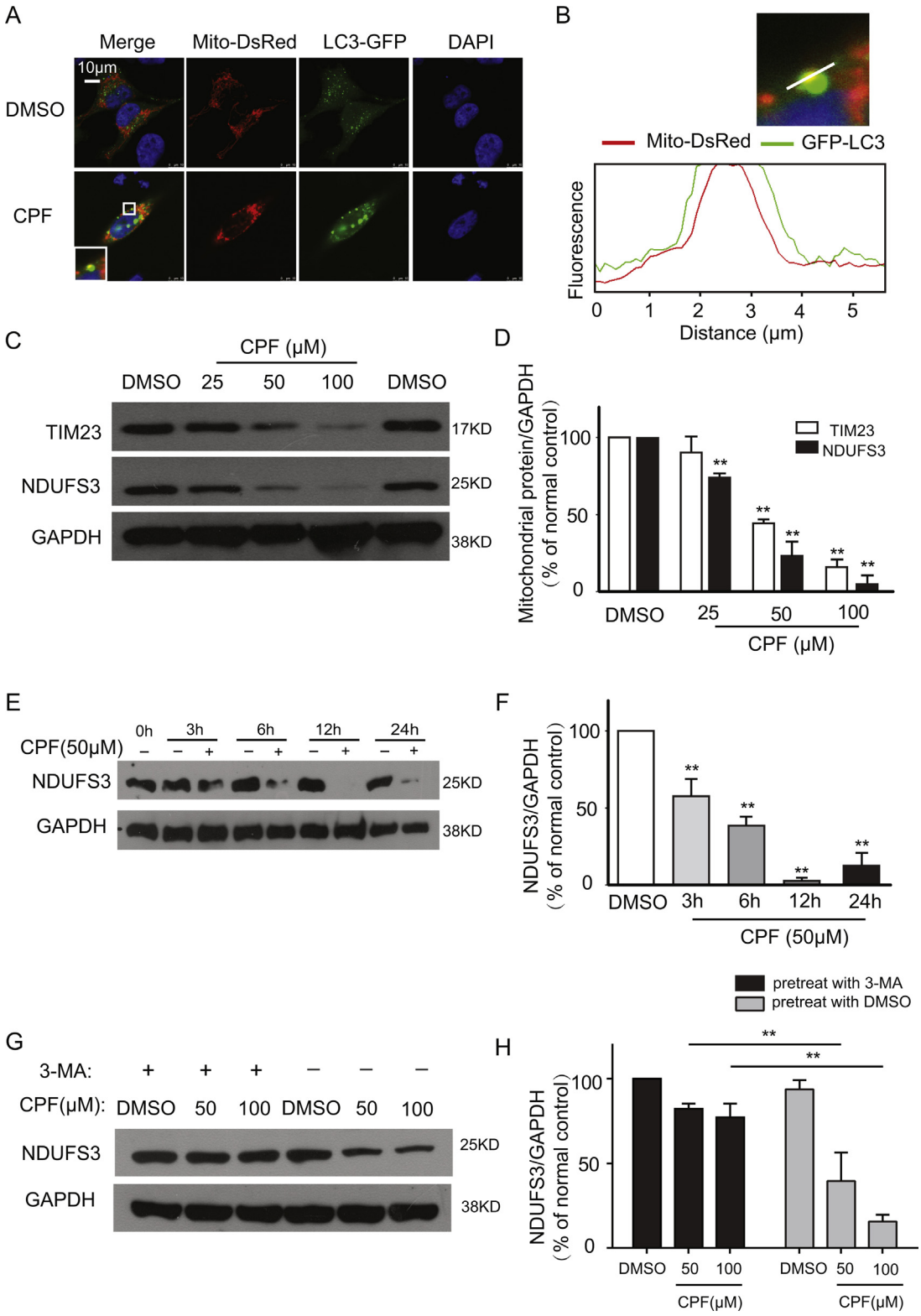

Fig. 3. CPF induces mitophagy in SH-SY5Y cells.
(A) Representative images (Scale bars, 10 μm). SH-SY5Y cells were transiently transfected with GFP-LC3 (green) and mito-DsRed (red) to label autophagosome and mitochondria, respectively. 24 h after transfection, the cells were treated with 50 μM CPF for 6 h. The distribution of GFP-LC3 and mito-DsRed was analyzed by microscopy. (B) Line profiles: colocalization of LC3-GFP and mito-Dsred was defined as overlapped red and green peaks. (C, D) Expression of mitochondrial proteins TIM23 and NDUFS3 in cells treated for 24 h with indicated concentrations of CPF. (C) Representative blots and (D) densitometric analysis of blots. (E, F) Expression of NDUFS3 in cells treated with 50 μM CPF exposure at indicated time points. (E) Representative blots and (F) densitometric analysis of blots. (G, H) Effect of 3-MA on NDUFS3 expression. Cells were pretreated with 3-MA (5 μM) or DMSO for 12 h before exposed to 50 μM CPF (or DMSO) for 24 h. (G) Representative blots and (H) densitometric analysis of blots. $^{**}p < 0.01$, with the respect to the control cells (DMSO).

showed that, similar to CCCP (carbonyl cyanide *m*-chlorophenylhydrazone) that has been implicated to cause mitochondrial depolarization, CPF significantly decreased the fluorescent signal of TMRE in SH-SY5Y cells, suggesting that CPF causes mitochondrial depolarization. Together, these findings demonstrate that CPF exposure induces mitochondrial damage and ROS generation.

3.3. CPF induces mitophagy in SH-SY5Y cells

In order to determine whether CPF exposure activates mitophagy in SH-SY5Y cells, we initially examined the colocalization of mitochondria with autophagosome by fluorescent microscopy. To this end, SH-SY5Y cells were transfected with LC3-GFP and mito-Dsred to label autophagosome and mitochondria, respectively. 24 h after transfection, the cells were then treated with

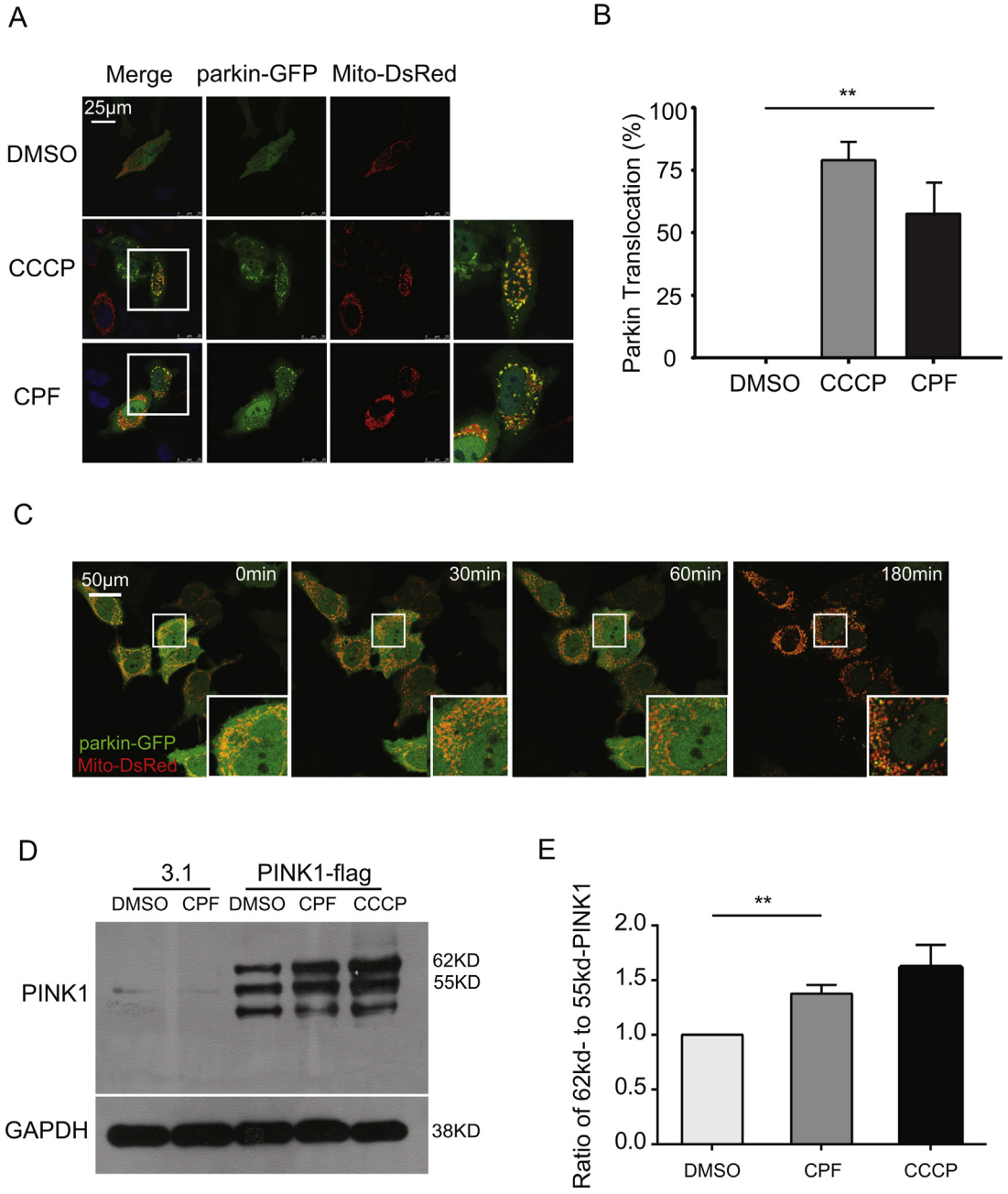

Fig. 4. CPF exposure promotes mitochondrial translocation of Parkin and stabilization of PINK1.
(A, B) SH-SY5Y cells were co-transfected with Parkin-GFP and mito-DsRed plasmids. 24 h after transfection, the cells were treated with 50 μM CPF for 6 h or 20 μM CCCP for 2 h as positive control. The distribution of Parkin-GFP (green) and mito-DsRed (red) was visualised by confocal microscopy. (A) Representative images (Scale bars, 25 μm). (B) Percentage of cells with mitochondrial Parkin-GFP. The number of cells with mitochondrial Parkin-GFP was normalized to total cells expressing both Parkin-GFP and mito-DsRed ($N = 3$, $n > 200$). (C) Time-course of Parkin translocation and mitochondrial fragmentation. Live cell imaging analysis was performed using an Ultra View Live Cell Imaging System after 50 μM CPF treatment, and representative images at indicated time points were presented. (D, E) Western blot analysis of PINK1 expression. SH-SY5Y cells were transfected with pcDNA3.1 or PINK1-flag for 24 h. Then the cells were treated with 50 μM CPF for 6 h or 20 μM CCCP for 2 h as positive control. (D) Representative blots and (E) densitometric analysis of blots. The vertical axis represents the ratio of full-length 62 kd-PINK1 to 55 kd-PINK1 normalized to negative control (DMSO). $^{**}p < 0.01$, with the respect to the control cells (DMSO).

50 μM CPF for 6 h. As shown in Fig. 3A and B, in control cells, LC3-GFP were evenly distributed. However, in CPF-treated cells, LC3-GFP aggregated and LC3-GFP puncta colocalized with mito-Dsred labeled mitochondria, which suggested mitophagy. We further determined the expression of mitochondrial proteins TIM23 and NDUFS3 by western blot analysis. As shown in Fig. 3C–F, CPF treatment resulted in concentration- and time-dependent decreases in the levels of mitochondrial proteins, like TIM23 and NDUFS3, which were confirmed by densitometry of immunoblots from three separate experiments. In order to confirm whether the reduction of mitochondrial proteins was resulted from the enhanced mitophagy, cells were treated with 3-MA, an inhibitor of autophagy, and then the expression of NDUFS3 was examined. As shown in Fig. 3G and H, 3-MA treatment markedly inhibited

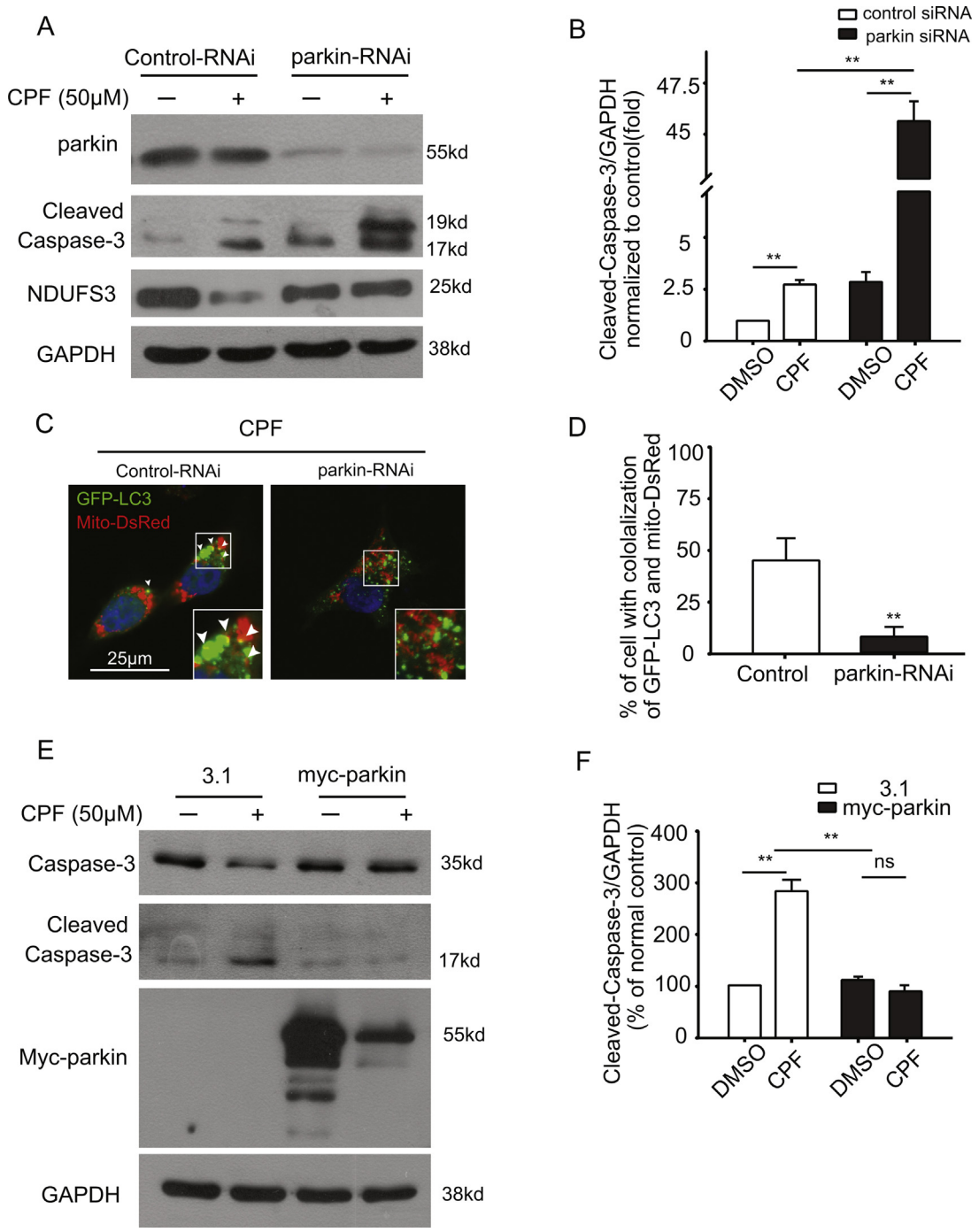

Fig. 5. The effect of knock down or overexpression of Parkin on the effects of CPF-induced apoptosis in SH-SY5Y cells.
(A, B) The effect of Parkin knockdown on CPF-induced apoptosis. 72 h after transfection with Parkin siRNA or control siRNA. SH-SY5Y cells were treated with 50 μM CPF for 24 h. (A) Representative blots and (B) densitometric analysis of blots. (C, D) 48 h after transfection with Parkin siRNA or control siRNA, SH-SY5Y cells were co-transfected with LC3-GFP (green) and mito-DsRed (red) plasmids for another 24 h, then the cells were treated with 50 μM CPF for 6 h before fixed for image analysis by confocal microscopy. (C) Representative images (Scale bars, 25 μm). (D) Percentage of cells containing colocalization of LC3-GFP (green) with mito-DsRed (red) ($N = 3$, $n > 200$). (E, F) The effect of overexpression of Parkin on CPF-induced apoptosis. SH-SY5Y cells were transfected with myc-Parkin or pcDNA3.1 as control. 24 h after transfection, the cells were treated with 50 μM CPF for 24 h. (E) Representative blots and (F) densitometric analysis of blots. $^{**}p < 0.01$, ns represents not significant, with the respect to the control group.

reduction of NDUFS3. Collectively, these results indicate that CPF exposure induces mitophagy in SH-SY5Y cells.

3.4. CPF-induced mitophagy is mediated by PINK1/Parkin pathway

Accumulating evidences demonstrate that PINK1/Parkin pathway is critical for autophagic degradation of damaged mitochondria (Novak, 2012). Therefore, we wanted to know whether CPF-induced mitophagy is PINK1/Parkin dependent. Initially, we determined whether CPF treatment caused mitochondrial accumulation of Parkin in SH-SY5Y cells. With regard to this, SH-SY5Y cells were transfected with Parkin-GFP plasmids and mito-DsRed plasmids, and then treated with 50 μM CPF for 6 h. As shown in Fig. 4A and B, similar to CCCP, CPF treatment also caused mitochondrial accumulation of Parkin-GFP. However, in control cells, Parkin-GFP distributed evenly and diffusely. Cell counting analysis revealed that >50% cells showed mitochondrial translocation of Parkin after CPF treatment. Live cell image analysis showed that after 50 μM CPF exposure, mitochondrial translocation of Parkin occurred within 3 h in SH-SY5Y cells (Fig. 4C). PINK1 stabilization on mitochondria is requisite for mitochondrial translocaiton of Parkin in mitophagy, so we examined the expression of PINK1 in SH-SY5Y cells treated with CPF by western blot analysis. As shown in Fig. 4D and E, CPF treatment dramatically increased the level of full length 62 KD PINK1. Taken together, these results suggest the involvement of PINK1/Parkin pathway in CPF-induced mitophagy in SH-SY5Y cells.

3.5. PINK1/Parkin-mediated mitophagy is protective for CPF-induced apoptosis

We then determined the role of mitophagy in CPF-induced apoptosis in SH-SY5Y cells. Firstly, we determined the effect of Parkin knockdown on CPF-induced apoptosis. We found that Parkin siRNA resulted in partial restoration of CPF-induced reduction of NDUFS3, and increase of CPF-induced cleavage of caspase-3 (Fig. 5A and B), and a decrease in the colocalization of LC3-GFP with mito-DsRed (Fig. 5C, and D). These results indicated that Parkin siRNA inhibited CPF-induced mitophagy and provided further evidence for the role of Parkin in CPF-induced mitophagy. Moreover, in response to Parkin siRNA, the increased level of cleaved caspase-3 caused by CPF also suggested that Parkin was protective against CPF-induced apoptosis. Furthermore, enhancing mitophagy through overexpression of Parkin before CPF treatment markedly decreased caspase-3 activation (Fig. 5E and F). Taken together, these results indicate that PINK1/Parkin-mediated mitophagy is cytoprotective for CPF-induced apoptosis.

4. Discussion

The present study demonstrated that CPF exposure induced PINK1/Parkin-mediated mitophagy, which was cytoprotective for CPF-induced apoptosis in SH-SY5Y cells. We showed that CPF treatment resulted in increased generation of ROS, mitochondria fragmentation and mitochondrial depolarization. Further studies showed that CPF exposure induced the colocalization of mitochondria with autophagosome, stabilizaiton of PINK1 and mitochondrial translocation of Parkin, indicating the induction of PINK1/Parkin-mediated mitophagy. Besides, Parkin knockdown was shown to inhibit CPF-induced mitophagy, and increased CPF-induced apoptosis, whereas overexpression of Parkin alleviated CPF-induced apoptosis through enhancing mitophagy. These results indicated mitophagy is cytoprotective against CPF-induced apoptosis.

Mitochondria are the major cellular source of ROS and also vulnerable targets of ROS (Cho et al., 2010; Liesa et al., 2009). Pesticides and environmental toxins such as rotenone and paraquat have been shown to induce ROS generation (Czerniczyniec et al., 2011; Wang et al., 2011; Xiong et al., 2012). CPF exposure was also reported to increase ROS generation in PC12 cells (Lee et al., 2012). Here, we showed that CPF exposure increased ROS generation in SH-SY5Y cells, further supporting the role of CPF in inducing ROS generation. Collectively, these findings indicate that the elevation of ROS production may be served as a common mechanism for pesticides induced-cell death.

Mitochondria are also highly dynamic organelle that is engaged in repeated cycles of fusion and fission. The maintenance of mitochondrial dynamics is essential for maintaining normal cellular function. Previous studies have shown that CPF exposure caused a concentration-dependent decrease in mitochondrial length, number and their movement in axons (Middlemore-Risher et al., 2011). Here, we demonstrate that CPF exposure results in significant mitochondrial fragmentation (Fig. 2A and B). Mitochondrial fragmentation is the result of enhanced fission and/or decreased fusion, but the mechanism of CPF-induced mitochondrial fragmentation remains poorly understood.

There is a complicated interplay between ROS and mitochondrial dynamic (Bhatt et al., 2013). Increased ROS is implicated to induce mitochondrial fragmentation which in turn can increase ROS generation (Westermann, 2010). Further investigation will be needed to determine whether increased ROS production is the cause of mitochondrial fragmentation of SH-SY5Y cells under CPF exposure. Mitochondrial fragmentation has been shown to regulate mitochondria-dependent apoptosis via increasing the insertion of pro-apoptotic proteins, such as Bax and Bak into mitochondria (Lee et al., 2012; Novak, 2012; Westermann, 2010). CFP-induced mitochondrial fragmentation might contribute to the incidence of apoptosis. So, blocking mitochondrial fragmentation by inhibiting mitochondrial fission or promoting fusion will provide a direct evidence for the role of mitochondrial fragmentation in CPF-induced apoptosis.

Accumulating studies have implicated the involvement of autophagy in various biological and pathological processes. For example, up-regulation of autophagy is implicated in infections, neurodegenerative and myodegenerative diseases, cardiomyopathies, and cancer (Martinez-Vicente and Cuervo, 2007). Recently, Park et al. (2013) showed that autophagy was activated during CPF treatment, and enhancing autophagy by rapamycin alleviated CPF-induced cell death, suggesting that autophagy is cytoprotective during CPF-induced cytotoxicity. Accumulation of damaged mitochondria causes excessive oxidative stress and cell death (Cho et al., 2010), so removal of damaged mitochondria may prevent cell death. Based on this conception, we hypothesized that mitophagy might contribute to the cytoprotective effects by removing damaged mitochondria. In mammalian cells, mitochondrial depolarization is the most well documented factor of mitophagy. For example, CCCP, a mitochondrial-uncoupling reagent, has been shown to induce mitophagy in different cell types. Moreover, it was reported that mitochondrial fragmentation is required for activation of mitophagy. However, mitochondrial fragmentation itself is not enough to induce mitophagy, which needs some other factors such as ROS generation and mitochondrial depolarization (Frank et al., 2012; Matsuda et al., 2010). In this study, we showed that CPF induced ROS generation and mitochondrial depolarization in SH-SY5Y cells. So, we hypothesized that CPF induced mitophagy. In supporting of this hypothesis, we have shown in this study, CPF exposure can induce mitophagy in SH-SY5Y cells, as manifested by the increased colocalization of LC3-GFP with mito-DSred (Fig. 3A and B), and decreased level of mitochondrial inner membrane proteins TIM23 and NDUFS3 (Fig. 3C–H). In addition, this is consistent with the conception

that ROS generation and mitochondrial depolarization is required for mitophagy activation.

PINK1/Parkin pathway is the most well documented signaling pathway in mitophagy. In response to mitochondrial depolarization, full length PINK1 accumulates on mitochondrial outer membrane, which then recruits Parkin to the damaged mitochondria. Once recruited, Parkin ubiquitinates various substrates to induce and promote autophagic removal of damaged mitochondria (Geisler et al., 2010; Jin et al., 2010; Jin and Youle, 2012). Our study demonstrate that PINK1/Parkin pathway is involved in CPF-induced mitophagy, which is supported by the following evidences. Firstly, CPF treatment increased the level of full length PINK1 (Fig. 4D and E); Secondly, CPF exposure induced the mitochondrial translocation of Parkin (Fig. 4A–C). In addition to PINK1/Parkin, several other proteins, such as such as BNIP3 (Bcl-2/adenovirus E1B 19kD-interacting protein 3) and Nix, have been also implicated to mediate mitophagy. So, it will be interesting to determine whether these proteins are also involved in CPF-induced mitophagy.

Substantial evidence has implicated that mitophagy plays a protective role in various pathological conditions by removing damaged mitochondria. In this study, we found that inhibition of mitophagy by Parkin knockdown increased CPF-induced apoptosis (Fig. 5A–D). However, overexpression of Parkin significantly suppressed CPF-induced apoptosis in SH-SY5Y cells (Fig. 5E and F). These findings implicate that mitophagy plays a protective role in CPF-induced cell death.

Overall, our study demonstrated for the first time that CPF exposure induces PINK1/Parkin-mediated mitophagy, which alleviates CPF-induced apoptosis. These findings will further our understanding on the molecular mechanism of CPF-related neurological disorders. Moreover, the findings in present study also suggest that enhancing mitophagy provides a potential therapeutic strategy for CPF-induced neurological disorders.

Conflict of interests

The authors declare that there are no conflicts of interest in the present work.

Acknowledgments

This work was supported by Construction Fund for Key Subjects of Hunan Province (2012) and United Bank of Switzerland-Optimus Foundation (GIFTS ID 6102). We are grateful to academician XIA Jiahui and the staff from the State Key Laboratory of Medical Genetics at Central South University for their excellent technical assistance. Special thanks should go to JIA Sujie for providing language help and writing assistance in proof reading the article.

Appendix A. Supplementary data

Supplementary data associated with this article can be found, in the online version, at http://dx.doi.org/10.1016/j.tox.2015.06.003.

References

Aldridge, J.E., Levin, E.D., Seidler, F.J., Slotkin, T.A., 2005. Developmental exposure of rats to chlorpyrifos leads to behavioral alterations in adulthood, involving serotonergic mechanisms and resembling animal models of depression. Environ. Health Perspect. 113, 527–531.

Bhatt, M.P., Lim, Y.C., Kim, Y.M., Ha, K.S., 2013. C-peptide activates ampkalpha and prevents ros-mediated mitochondrial fission and endothelial apoptosis in diabetes. Diabetes 62, 3851–3862.

Bouchard, M.F., Chevrier, J., Harley, K.G., Kogut, K., Vedar, M., Calderon, N., et al., 2011. Prenatal exposure to organophosphate pesticides and iq in 7-year-old children. Environ. Health Perspect. 119, 1189–1195.

Canadas, F., Cardona, D., Davila, E., Sanchez-Santed, F., 2005. Long-term neurotoxicity of chlorpyrifos: Spatial learning impairment on repeated acquisition in a water maze. Toxicol. Sci. 85, 944–951.

Cho, D.H., Nakamura, T., Lipton, S.A., 2010. Mitochondrial dynamics in cell death and neurodegeneration. Cell. Mol. Life Sci. 67, 3435–3447.

Czerniczyniec, A., Karadayian, A.G., Bustamante, J., Cutrera, R.A., Lores-Arnaiz, S., 2011. Paraquat induces behavioral changes and cortical and striatal mitochondrial dysfunction. Free Radical Biol. Med. 51, 1428–1436.

Engel, S.M., Berkowitz, G.S., Barr, D.B., Teitelbaum, S.L., Siskind, J., Meisel, S.J., et al., 2007. Prenatal organophosphate metabolite and organochlorine levels and performance on the brazelton neonatal behavioral assessment scale in a multiethnic pregnancy cohort. Am. J. Epidemiol. 165, 1397–1404.

Engel, S.M., Wetmur, J., Chen, J., Zhu, C., Barr, D.B., Canfield, R.L., et al., 2011. Prenatal exposure to organophosphates, paraoxonase 1, and cognitive development in childhood. Environ. Health Perspect. 119, 1182–1188.

Eskenazi, B., Marks, A.R., Bradman, A., Harley, K., Barr, D.B., Johnson, C., et al., 2007. Organophosphate pesticide exposure and neurodevelopment in young mexican-american children. Environ. Health Perspect. 115, 792–798.

Frank, M., Duvezin-Caubet, S., Koob, S., Occhipinti, A., Jagasia, R., Petcherski, A., et al., 2012. Mitophagy is triggered by mild oxidative stress in a mitochondrial fission dependent manner. Biochim. Biophys. Acta 1823, 2297–2310.

Freire, C., Koifman, S., 2012. Pesticide exposure and Parkinson's disease: epidemiological evidence of association. Neurotoxicology 33, 947–971.

Geisler, S., Holmstrom, K.M., Treis, A., Skujat, D., Weber, S.S., Fiesel, F.C., et al., 2010. The PINK1/Parkin-mediated mitophagy is compromised by PD-associated mutations. Autophagy 6, 871–878.

Gupta, S.C., Mishra, M., Sharma, A., Deepak Balaji, T.G., Kumar, R., Mishra, R.K., et al., 2010. Chlorpyrifos induces apoptosis and DNA damage in drosophila through generation of reactive oxygen species. Ecotoxicol. Environ. Saf. 73, 1415–1423.

Jin, S.M., Lazarou, M., Wang, C., Kane, L.A., Narendra, D.P., Youle, R.J., 2010. Mitochondrial membrane potential regulates PINK1 import and proteolytic destabilization by PARL. J. Cell Biol. 191, 933–942.

Jin, S.M., Youle, R.J., 2012. PINK1- and Parkin-mediated mitophagy at a glance. J. Cell Sci. 125, 795–799.

Lee, J.E., Park, J.H., Shin, I.C., Koh, H.C., 2012. Reactive oxygen species regulated mitochondria-mediated apoptosis in PC12 cells exposed to chlorpyrifos. Toxicol. Appl. Pharmacol. 263, 148–162.

Liesa, M., Palacin, M., Zorzano, A., 2009. Mitochondrial dynamics in mammalian health and disease. Physiol. Rev. 89, 799–845.

Martinez-Vicente, M., Cuervo, A.M., 2007. Autophagy and neurodegeneration: when the cleaning crew goes on strike. Lancet Neurol. 6, 352–361.

Matsuda, N., Sato, S., Shiba, K., Okatsu, K., Saisho, K., Gautier, C.A., et al., 2010. PINK1 stabilized by mitochondrial depolarization recruits Parkin to damaged mitochondria and activates latent Parkin for mitophagy. J. Cell Biol. 189, 211–221.

Meissner, C., Lorenz, H., Weihofen, A., Selkoe, D.J., Lemberg, M.K., 2011. The mitochondrial intramembrane protease parl cleaves human PINK1 to regulate PINK1 trafficking. J. Neurochem. 117, 856–867.

Middlemore-Risher, M.L., Adam, B.L., Lambert, N.A., Terry Jr., A.V., 2011. Effects of chlorpyrifos and chlorpyrifos-oxon on the dynamics and movement of mitochondria in rat cortical neurons. J. Pharmacol. Exp. Ther. 339, 341–349.

Narendra, D., Tanaka, A., Suen, D.F., Youle, R.J., 2008. Parkin is recruited selectively to impaired mitochondria and promotes their autophagy. J. Cell Biol. 183, 795–803.

Novak, I., 2012. Mitophagy: a complex mechanism of mitochondrial removal. Antioxid. Redox Signaling 17, 794–802.

Park, J.H., Lee, J.E., Shin, I.C., Koh, H.C., 2013. Autophagy regulates chlorpyrifos-induced apoptosis in SH-SY5Y cells. Toxicol. Appl. Pharmacol. 268, 55–67.

Pidoux, G., Witczak, O., Jarnaess, E., Myrvold, L., Urlaub, H., Stokka, A.J., et al., 2011. Optic atrophy 1 is an a-kinase anchoring protein on lipid droplets that mediates adrenergic control of lipolysis. EMBO J. 30, 4371–4386.

Qiao, D., Seidler, F.J., Slotkin, T.A., 2001. Developmental neurotoxicity of chlorpyrifos modeled in vitro: comparative effects of metabolites and other cholinesterase inhibitors on DNA synthesis in PC12 and C6 cells. Environ. Health Perspect. 109, 909–913.

Rauh, V., Arunajadai, S., Horton, M., Perera, F., Hoepner, L., Barr, D.B., et al., 2011. Seven-year neurodevelopmental scores and prenatal exposure to chlorpyrifos, a common agricultural pesticide. Environ. Health Perspect. 119, 1196–1201.

Saulsbury, M.D., Heyliger, S.O., Wang, K., Round, D., 2008. Characterization of chlorpyrifos-induced apoptosis in placental cells. Toxicology 244, 98–110.

Wang, L., Sun, Y., Asahi, M., Otsu, K., 2011. Acrolein, an environmental toxin, induces cardiomyocyte apoptosis via elevated intracellular calcium and free radicals. Cell Biochem. Biophys. 61, 131–136.

Westermann, B., 2010. Mitochondrial fusion and fission in cell life and death. Nat. Rev. Mol. Cell Biol. 11, 872–884.

Whyatt, R.M., Rauh, V., Barr, D.B., Camann, D.E., Andrews, H.F., Garfinkel, R., et al., 2004. Prenatal insecticide exposures and birth weight and length among an urban minority cohort. Environ. Health Perspect. 112, 1125–1132.

Xiong, N., Long, X., Xiong, J., Jia, M., Chen, C., Huang, J., et al., 2012. Mitochondrial complex I inhibitor rotenone-induced toxicity and its potential mechanisms in Parkinson's disease models. Crit. Rev. Toxicol. 42, 613–632.